IJCSE International Journal of Computer Sciences and Engineering Open Access
Research Paper Vol.-6, Issue-7, July 2018 E-ISSN: 2347-2693

Fusion of CT and MR Scans of lumbar Spine Using Discrete Image Transforms

B.N. Palkar[1*], D. Mishra[2]

[1, 2*]Computer Department, MPSTME, NMIMS, Mumbai, India

[*]*Corresponding Author: bhaktiraul@somaiya.edu*

Available online at: www.ijcseonline.org

Accepted: 20/July/2018, Published: 31/July/2018

Abstract— Fused Medical image of different modalities produces more explanatory image compared to the input images considered separately. This is useful for the medical practitioners for better treatment planning for the patient. In this paper we have experimented with various mathematical transforms to fuse Computed Tomography (CT) and Magnetic Resonance imaging (MRI) scans of lumber spine. CT images mainly depict more information related to bones of the scanned body part whereas MR images provide the details of soft tissues more clearly. CT and MR images have been aligned / registered with each other to achieve better fusion output. Ten cases have been considered for generating the image datasets for experiments. All the fused results are compared using four quantitative quality assessment parameters: entropy, standard deviation, fusion factor and fusion symmetry and also by qualitative way. Quantitative and qualitative assessment indicates that fused images generated by fast walsh hadamard transform carry symmetrically good amount of information from both images and of good contrast. These images can be used for better patient treatment planning by medical practitioners.

Keywords— Medical image processing; image fusion, image transforms, CT, MR

I. Introduction

Medical Image Analysis Software Market is anticipated to grow rapidly due to increasing chronic diseases [online Grand View Research May 2018]. ‘Medical image fusion’ is developing branch of ‘medical image analysis’ which deals with integrating relevant information presented in multiple medical images into one image which is more informative than input images. There are multiple Mono-modal and multi-modal images available of the same body part. These images of the same body part can be fused. Mono-modal images are fused to observe pre and post-operative difference in the image scans. Multi-modal images are fused when single modality image does not help clinicians in taking diagnostic decisions. Computed Tomography (CT) scans provide information about bone structures/ alignment. Magnetic Resonance Image (MRI) scans provide soft tissue details. So the fused image of CT and MR scanned images depicts both bones and soft tissues details. CT and MR images are captured using different image acquisition devices, at different times with different viewpoints. This presents the unaligned images of different modalities. This is why the process of ‘registration’ needs to be performed on input CT and MR images to bring them into same pixel coordinated position. This helps for better fusion of multiple images of different modality. In recent times, many researchers have worked on ‘image fusion’ in general [2]. Image fusion is done on three levels: pixel, feature and decision. In Pixel level fusion original pixel intensities are fused. Feature level fusion- objects are fused based on extracted features. Decision level fusion techniques are mostly based on fuzzy logic. Pixel level fusion techniques are of two types: spatial domain and frequency domain. Spatial domain advocates the fusion of the original pixel values of images. There are various spatial domain approaches such as Averaging, minimum, maximum, min-max, block replace [3,4], weighted average [5], HIS [6], Brovey [7], principal component analysis (PCA) [8] and guided filtering [9]. Spatial domain techniques suffer from low contrast or colour distortion. Frequency domain techniques are divided into two types: Fusion based on pyramids [10-17] and fusion based on discrete image transforms. Fused image generated by pyramid based methods carry blocking effect. These images sometimes carry redundant information also. Frequency domain fusion techniques are based on wavelets [18-21], stationary wavelets [22-24], Kekre’s wavelet transform (KWT) [25,26], Kekre’s Hybrid Wavelet Transform (KHWT) [27-29]. Wavelet based methods provide better results than pyramid based fusion. Localization and multi-directional features of wavelet transform make it superior to pyramid transform. But discrete wavelet transform has two major shortcomings - shift variance and lack of directionality [30]. The dual tree complex wavelet transform (DT-CWT) came into existence to deal with the shortcomings of wavelet transform. DT-CWT is shift invariant. It is also applied for image fusion [31]. Curvelets transform is also used for fusion [32] to show curves and edges more accurately. Contourlet transform can easily extract geometrical structure from the images [33]. But it is not shift-invariant. The non-subsampled Contourlet transform (NSCT) [34] is more time consuming. In recent years, Shearlet transform [35], edge-preserving filtering [36-38], anisotropic heat diffusion [39], log-Gabor transform [40], and support value transform [41-42] also have been applied for multi scale decomposition based fusion. Outcome of all wavelet based fusion techniques depend on the number of decomposition levels. Lessor number of decomposition levels does not guarantee spatial quality of the fused images. Excessive number of decomposition levels may increase execution time and decrease performance. DCT transform has also been applied to perform pixel based image fusion [43] but it is not compared with performance of other image fusion methods. Also none of the authors have used discrete image transforms other than DCT to perform fusion. In this paper we have used Fast Fourier Transform, Discrete Sine Transform, Discrete Slant transform, Fast Walsh Hadamard Transform and Discrete Hartley Transform to fuse CT and MR scans of lumbar spine images. Performances of fusion achieved after applying these transforms are compared both subjectively (by the designated medical practitioner expert) and objectively with other fusion methods. All fusion algorithms have been experimented with ten patient cases. The cases are taken from dataset1 of 'SpineWeb' which is publicly available online [44]. This paper is organized as follows: Section II gives explains image fusion using various mathematical transforms. Section III discusses and analyses the various results obtained from each experiments conducted. Section IV gives closing remark as conclusion. Section V shows acknowledgement.

II. FUSION USING IMAGE TRANSFORMS

In this paper Fast Fourier transform (FFT), Discrete cosine transform (DCT), Discrete sign transform (DST), Discrete Hartley Transform (DHT), Slant Transform and Fast Walsh-hadamard transform (FWHT) are used to perform fusion. Figure 2 demonstrates the method 'fusion using discrete transforms'. Both the input images are passed through pre-processing stage where contrasts of both the images are enhanced using contrast limited adaptive histogram equalization technique. In the second stage of 'registration', CT image is aligned with MR image using control point based registration technique. In all the image pairs that are considered for fusion, CT images cover lesser part of the spine as compared to MR images. Because of this MR image is considered as fixed image and CT image is treated as moving image. Using Control point based registration technique; user has to select manually matching landmark points from fixed and moving images. From the positions of these control points, a geometric transformation is inferred. This geometric transformation is then applied on moving image to bring both the images in same pixel coordinated position. Control point based registration technique is useful when prioritization of the alignment of specific features is necessary. While registering two multi-modal lumbar spine images, we can focus on the alignment of vertebrae, disc and spine while selecting control points. In the third stage, MR image and registered CT image are transformed into frequency domain using six transforms. Fused image of CT and MR images is expected to show soft tissues as well as bone structures. So, 'Average' fusion rule is used to fuse two transformed images. Appropriate inverse transform is invoked in the end to get the fused image. All the methods have been tested on ten patient cases from dataset1 of 'SpineWeb' [44] wherein all the images are of size 512×512.

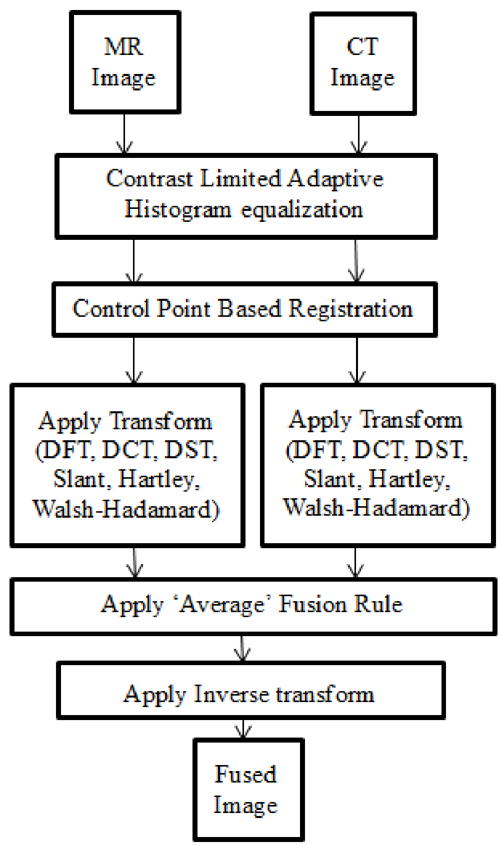

Figure 1: Fusion of CT and MR images

III. RESULTS AND DISCUSSION

We have compared results obtained by our method with other well-known approaches for fusion namely Principal component analysis (PCA) [8], Stationary Wavelet Transform (SWT) [22-24], Discrete Cosine Transform-Laplacian Pyramid (DCT-LP) [11], Discrete Wavelet

Transform (DWT)[18] and Dual tree complex wavelet Transform (DT-CWT) [31].

A. Experimental settings and dataset

All the fusion methods have been experimented with ten CT and T2 weighted MR image pairs of different patients' cases within the age group of 30 to 60 years, male and female. All the images are of size 512×512. Table 1 shows the lumber spine disorders that these 10 patients suffer from. Two different images can be fused only if the images are aligned with each other. Therefore we have aligned CT image with MR image for every case using control point based registration technique.

B. Experimental results

Fused images obtained using all the methods are presented in this section. We have shown results in visual form for only two cases and in tabular form for ten cases.

Table 1: Case Details

Case No.	Type
1	Prolapse Disk, Disk thinning, Bulging Disk
2	Spondylolisthesis, Degenerative disk and osteophyte
3	Spinal stenosis, disk thinning, herniation, osteophyte formation
4	Spondylolisthesis
5	Disk Herniation
6	Degenerative disk, Osteophyte
7	Spinal stenosis, Disk Herniation
8	Disk thinning, Disk Herniation
9	Osteophyte formation
10	Osteophyte formation

Fig. 2 shows fusion results for case 1. Fig. 3 shows fusion results for case 2. Fused images of ten cases have been evaluated visually by well-known orthopaedic surgeon for qualitative assessment. If two fused images are similar, our eyes cannot decide which image is better. So, we have also added quantitative assessment by evaluating all fused results using four quality parameters: entropy (E), standard deviation (SD), fusion factor (FF) and fusion symmetry (FS) [8]. Entropy gives information about information content in the image. High value of entropy indicates high information content. Standard deviation (SD) gives information about contrast in the image. High value of standard deviation indicates high contrast. Both fusion factor and fusion symmetry are based on mutual information between source images and fused image. A high value of fusion factor indicates that it has relatively good amount of information from both images. Fusion symmetry (FS) gives information about degree of symmetry in the information content from two input images. Fusion symmetry should be as low as possible. Values of these parameters, for all the methods, are tabulated in Tables 2–11, corresponding to all CT and MR image pairs used in our experiments. The best results in each table are highlighted in bold face. To understand the difference in fused results obtained using all the methods, we have used bar chart to represent quality parameters values.

C. Analysis and Observations

- From tables 2- 11, we could observe that DT-CWT has shown highest entropy (E) values for all the 10 patient cases which indicates that fused image generated by DT-CWT holds highest amount of information as compared to other methods. Apart from DT-CWT, DCT-LP and PCA are other two methods which have shown entropy values very near to the entropy values of DT-CWT. But at the same time fused images shown by DT-CWT and DCT-LP are low contrast images which make them difficult to interpret.
- From tables 2- 11, we could observe that DT-CWT which has shown highest entropy values for all ten cases has shown worst standard deviation values for 9 cases. This indicates that even though DT-CWT fused images carry some information because of low contrast the fused images become unusable. PCA has shown best SD values for cases 1,3,5,6 and 7. Fast Walsh hadamard transform has shown best SD values for cases 2 and 8. Slant transform has shown best SD values for cases 9 and 10. However SD values of DFT, DCT, DST, Slant, fast wash hadamard and Hartley transforms have shown almost same values. That means fused images shown by all basic transforms and PCA are good contrast images.
- From tables 2- 11, we could observe that Fast Walsh Hadamard Transform has shown best fusion factor (FF) values for cases 1, 2 4,7,8,9 and 10. PCA has shown best FF values for cases 3, 5 and 6. Fusion factor values of DFT, DCT, DST, Slant, Hartley transform and PCA are very near to the values of fast walsh hadamard transform. FF values of DT-CWT are worst for all ten cases. Values of DCT-LP are also near to values of DT-CWT. This indicates that FWHT and sometimes PCA carry relatively good amount of information from both the images as compared to other transforms. DT-CWT and DCT-LP do not hold information from both the images.

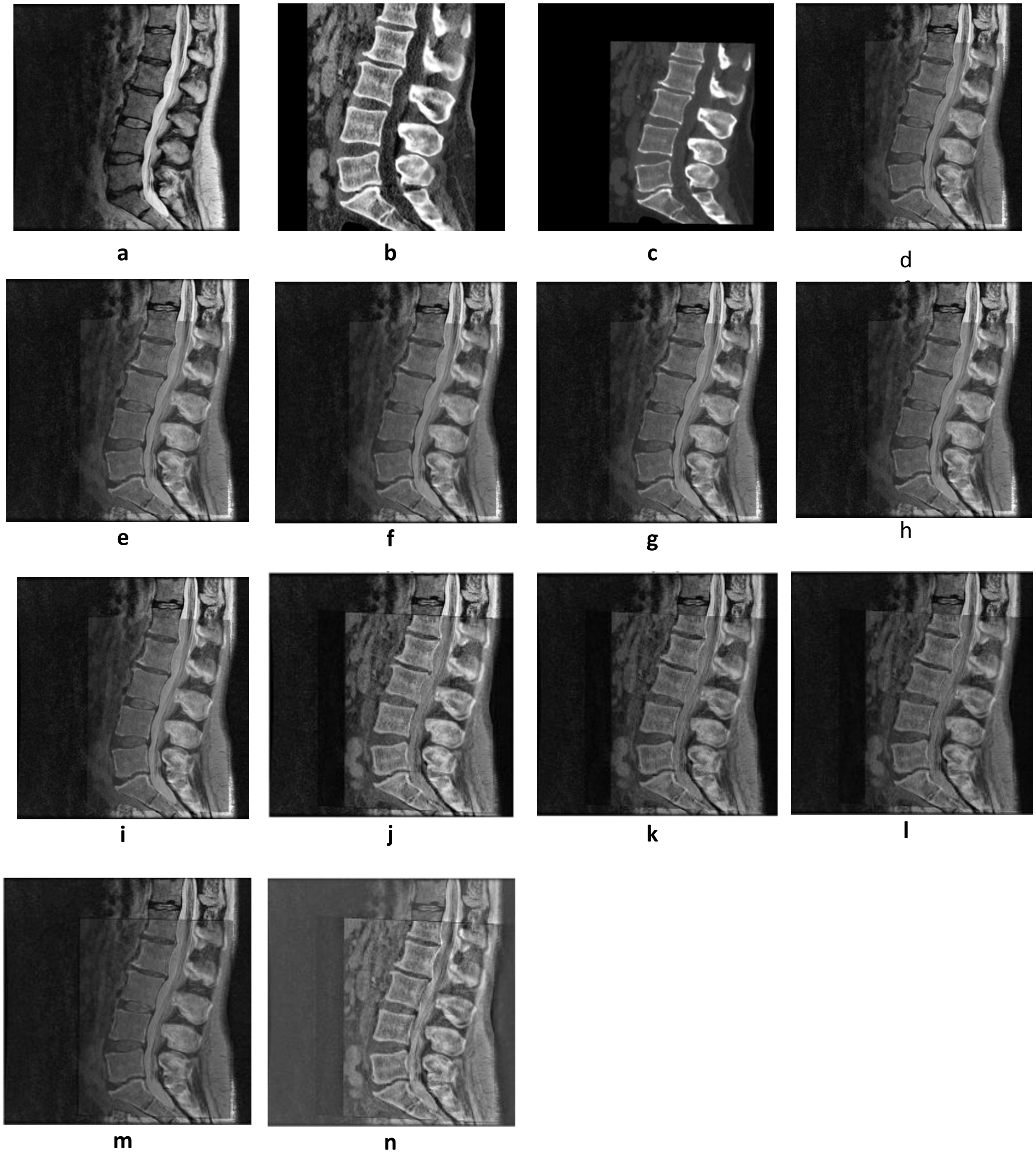

Figure 2: a)MR image, b)CT Image, c) Registered CT image, d)DFT fused image, e)DCT Fused image, f)DST Fused Image, g) Slant Fused Image, h)Fast Walsh-Hadamard Fused Image, i)Hartley Fused Image, j)PCA Fused Image, k) SWT Fused Image, l) DCT-LP Fused Image, m)DWT Fused Image, n)DT-CWT Fused Image.

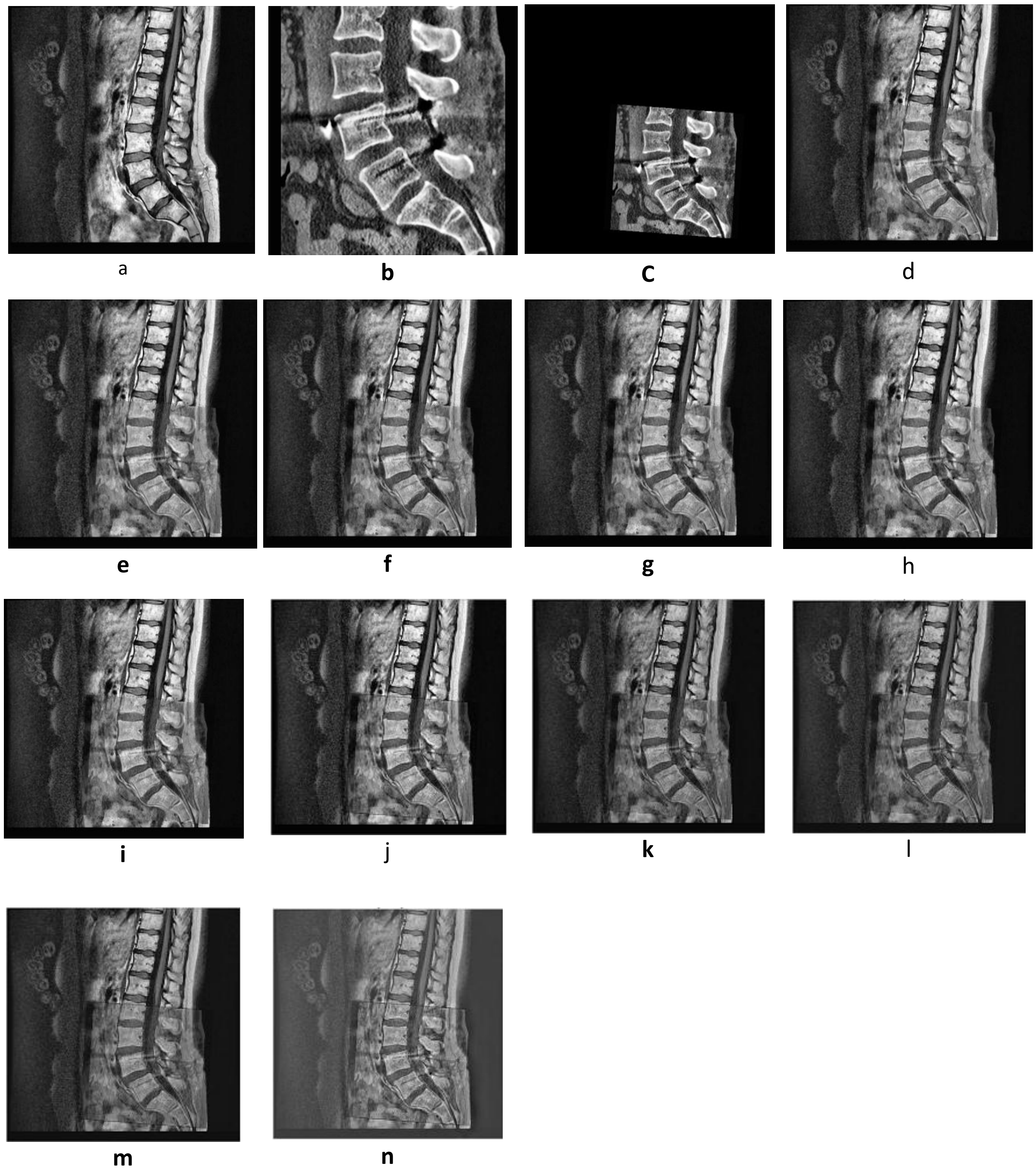

Figure 3: a)MR image, b)CT Image, c) Registered CT image, d)DFT fused image, e)DCT Fused image, f)DST Fused Image, g) Slant Fused Image, h)Hadamard Fused Image, i)Hartley Fused Image, j)PCA Fused Image, k) SWT Fused Image, l) DCT-LP Fused Image, m)DWT Fused Image, n)DT-CWT Fused Image.

Table 2:Case1- Quantitative assessment

Method	Entropy (High)	Standard Deviation (High)	Fusion Factor (High)	Fusion Symmetry (Low)
DFT	7.2571	10.0439	7.3334	0.0327
DCT	7.2569	10.0393	7.3300	0.0331
DST	7.2563	10.0379	7.3374	0.0330
Slant	7.2562	10.0365	7.3345	0.0329
FWHT	7.2514	10.0529	**7.4098**	**0.0284**
Hartley	7.2540	10.0380	7.3392	0.0331
PCA	7.2704	**10.1070**	7.2741	0.0562
SWT	7.2699	10.0977	7.0455	0.0587
DCT-LP	7.2800	10.0972	6.3453	0.0742
DWT	7.2583	10.0878	6.9819	0.0627
DT-CWT	**7.3567**	9.7041	4.6166	0.0890

Table 3: Case2- Quantitative assessment

Method	Entropy (High)	Standard Deviation (High)	Fusion Factor (High)	Fusion Symmetry (Low)
DFT	6.8544	10.6109	7.3802	0.0432
DCT	6.8536	10.6009	7.3784	0.0443
DST	6.8536	10.6057	7.3799	0.0443
Slant	6.8540	10.6059	7.3727	0.0437
FWHT	6.8547	10.6187	**7.4004**	**0.0420**
Hartley	6.8535	10.6059	7.3741	0.0437
PCA	6.9010	**10.4020**	7.1275	0.0630
SWT	6.8961	10.5889	6.9196	0.0496
DCT-LP	7.0458	10.5921	5.9352	0.0622
DWT	6.8822	10.5709	6.8854	0.0554
DT-CWT	**7.2323**	10.1969	4.4105	0.0525

Table 4: Case 3- Quantitative assessment

Method	Entropy (High)	Standard Deviation (High)	Fusion Factor (High)	Fusion Symmetry (Low)
DFT	7.0922	9.6330	6.8979	0.0716
DCT	7.0918	9.6936	6.9237	0.0706
DST	7.0907	9.7022	6.8993	0.0719
Slant	7.0920	9.7038	6.9140	0.0712
FWHT	7.0866	9.6434	6.9532	**0.0677**
Hartley	7.0891	9.7002	6.8938	0.0719
PCA	7.1746	**9.7849**	**7.1929**	0.1048
SWT	7.1236	9.7032	6.5931	0.0877
DCT-LP	7.1347	9.7040	6.1754	0.1143
DWT	7.1153	9.6969	6.8095	0.1068
DT-CWT	**7.1931**	9.2872	4.4758	0.0882

Table 5: Case 4-- Quantitative assessment

Method	Entropy (High)	Standard Deviation (High)	Fusion Factor (High)	Fusion Symmetry (Low)
DFT	6.5697	9.4201	8.5184	0.0293
DCT	6.5693	9.4157	8.5197	0.0296
DST	6.5692	9.4180	8.5044	0.0304
Slant	6.5696	9.4180	8.5082	0.0300
FWHT	6.5681	9.4249	**8.5710**	**0.0268**
Hartley	6.5696	9.4175	8.5106	0.0302
PCA	6.6411	9.3853	8.3848	0.0531
SWT	6.6261	9.4262	7.9987	0.0414
DCT-LP	6.6909	9.4199	7.1243	0.0597
DWT	6.6243	**9.4561**	7.9195	0.0496
DT-CWT	**6.7366**	9.1548	5.4836	0.0379

Table 6: Case 5-- Quantitative assessment

Method	Entropy (High)	Standard Deviation (High)	Fusion Factor (High)	Fusion Symmetry (Low)
DFT	6.7175	10.1000	5.5947	0.0304
DCT	6.7204	10.0807	5.6243	0.0329
DST	6.7158	10.0909	5.5941	0.0303
Slant	6.7169	10.0940	5.6012	0.0305
FWHT	6.7116	10.1083	5.6413	0.0325
Hartley	6.7128	10.0864	5.5924	0.0295
PCA	6.7938	**10.2613**	**5.6916**	0.0141
SWT	6.7703	10.0885	5.3445	0.0125
DCT-LP	6.9100	10.0902	4.8182	**0.0017**
DWT	6.7792	10.0792	5.3228	0.0058
DT-CWT	**7.1555**	9.8338	4.5891	0.0053

Table 7: Case 6-- Quantitative assessment

Method	Entropy (High)	Standard Deviation (High)	Fusion Factor (High)	Fusion Symmetry (Low)
DFT	7.4581	10.2283	5.7224	0.0058
DCT	7.4572	10.2031	5.7442	0.0076
DST	7.4564	10.2131	5.7117	**0.0048**
Slant	7.4569	10.2166	5.7152	0.0050
FWHT	7.4571	10.2415	5.7901	0.0115
Hartley	7.4563	10.2134	5.7137	0.0052
PCA	7.6294	**10.5483**	**8.3313**	0.1681
SWT	7.5121	10.2073	5.5691	0.0574
DCT-LP	7.5374	10.2144	4.4160	0.1017
DWT	7.4979	10.2627	5.4477	0.0698
DT-CWT	**7.6622**	10.3523	3.3991	0.1278

Table 8: Case 7-Quality Parameters

Method	Entropy (High)	Standard Deviation (High)	Fusion Factor (High)	Fusion Symmetry (Low)
DFT	7.4751	9.9833	9.9482	0.0014
DCT	7.4745	9.9733	9.9531	0.0013
DST	7.4743	9.9773	9.9509	0.0014
Slant	7.4744	9.9798	9.9515	0.0015
FWHT	7.4748	9.9887	**9.9550**	0.0020
Hartley	7.4744	9.9770	9.9481	0.0015
PCA	7.5205	**10.0105**	9.7444	0.0027
SWT	7.5327	9.9629	9.5081	**0.0012**
DCT-LP	7.5504	9.9611	7.9761	0.0077
DWT	7.5050	9.9306	9.4392	0.0066
DT-CWT	**7.6285**	9.9196	5.5777	0.0131

Table 9: Case 8-Quality Parameters

Method	Entropy (High)	Standard Deviation (High)	Fusion Factor (High)	Fusion Symmetry (Low)
DFT	7.2646	9.4550	10.0127	0.0080
DCT	7.2655	9.4591	10.0148	0.0080
DST	7.2650	9.4554	10.0129	0.0080
Slant	7.2655	9.4571	10.0156	0.0080
FWHT	7.2666	9.4628	**10.0323**	0.0086
Hartley	7.2652	**9.5035**	10.0142	0.0080
PCA	7.3063	9.4591	9.7565	0.0074
SWT	7.3117	9.4600	9.6437	0.0046
DCT-LP	7.3640	9.4565	8.6159	**0.0038**
DWT	7.3121	9.4987	9.6046	0.0042
DT-CWT	**7.4364**	9.1987	7.3804	0.0081

Table 10: Case 9-Quality Parameters

Method	Entropy (High)	Standard Deviation (High)	Fusion Factor (High)	Fusion Symmetry (Low)
DFT	7.3891	9.6470	11.8175	0.0392
DCT	7.3895	9.6467	11.8073	0.0393
DST	7.3890	9.6427	11.8108	0.0394
Slant	7.3882	**9.6531**	11.4940	0.0410
FWHT	7.3875	9.5981	**11.8218**	**0.0386**
Hartley	7.3882	9.6520	11.4979	0.0411
PCA	7.4117	9.5497	11.3186	0.0473
SWT	7.3986	9.6478	10.9609	0.0465
DCT-LP	7.4072	9.6439	9.8501	0.0621
DWT	7.3997	9.6170	10.9591	0.0527
DT-CWT	**7.4422**	9.4694	7.5139	0.0666

Table 11: Case 10-Quality Parameters

Method	Entropy (High)	Standard Deviation (High)	Fusion Factor (High)	Fusion Symmetry (Low)
DFT	6.7147	9.4719	9.9852	0.0180
DCT	6.7139	9.5168	9.9771	0.0183
DST	6.7142	9.5187	9.9794	0.0183
Slant	6.7143	**9.5190**	9.9783	0.0183
FWHT	6.7152	9.4741	**9.9929**	**0.0179**
Hartley	6.7143	9.5186	9.9779	0.0183
PCA	6.7221	9.4508	9.7621	0.0312
SWT	6.7491	9.5051	9.5815	0.0218
DCT-LP	6.7639	9.4988	8.5997	0.0262
DWT	6.7292	9.4824	9.5756	0.0280
DT-CWT	**6.7957**	9.1746	6.7468	0.0215

- From tables 2- 11, we could observe that Fast Walsh Hadamard Transform has shown best fusion symmetry (FS) values for cases 1,2,34,9, and 10. In all other cases values of FWHT are very near to the best FS values. Fusion symmetry values of DFT, DCT, DST, Slant, and Hartley transform and PCA are very near to the values of fast Walsh hadamard transform.
- For qualitative analysis the results were shown to well-known orthopaedic surgeon. He has observed that all ten cases cover various lumber spine disorders. Fused images obtained using SWT, DWT, DCT-LP and DT-CWT are low contrast images as compared to other methods. Performance of all other transforms DFT, DCT, DST, Slant, FWHT, Hartley and PCA are comparable. Particularly FWHT fused images can be used for further treatment planning.

IV. CONCLUSION

In this paper, we have used six discrete image transforms: DFT, DCT, DST, Slant, fast walsh, hadamard transform and Hartley transform to fuse CT and MR images for lumber spine disorders. The performance of these transforms are compared with other well-known fusion methods viz. PCA , SWT, DWT, DCT-LP and DT-CWT using quantitative and qualitative ways. For quantitative evaluation we used four parameters: entropy, standard deviation, fusion factor and fusion symmetry. It has been observed that fused images obtained using SWT, DWT, DCT-LP and DT-CWT are low contrast images as compared to other methods because of which both bony details and soft tissues cannot be clearly seen in fused images of these methods. Fused images generated by DFT, DCT, DST, slant, FWHT, Hartley and PCA are good contrast images. DT-CWT and DCT-LP do not carry information from both the images. Performance of DFT, DCT, DST, Slant, FWHT, and Hartley are comparable to

PCA. Particularly FWHT and sometimes PCA fused images carry symmetrically good amount of information from both the images as compared to other transforms. In all fusion factor, fusion symmetry, entropy and standard deviation help us in making the decision that fused image generated using FWHT can show maximum amount of information from both the images clearly. It also has good contrast which makes the image suitable for further treatment planning.

ACKNOWLEDGEMENT

Author would like to thank Dr. Arvind Bhave, MD, Orthopaedic Surgeon for evaluating results.

REFERENCES

[1] Medical image analysis software market worth
[2] https://www.grandviewresearch.com/press-release/global-medical-image-analysis-software-market (accessed 22 June 2018).
[3] Dhirendra Mishra and Bhakti Palkar. Article: Image Fusion Techniques: A Review. International Journal of Computer Applications130(9):7-13, November 2015. Published by Foundation of Computer Science (FCS), NY, USA.
[4] Jasiunas M. D., Kearney D. A., Hopf J. (2002) Image Fusion for Uninhabited Airborne Vehicles Proceedings of IEEE International Conference on Field Programmable Technology: 348-351.
[5] Dong, J., Zhuang, D., Huang, Y., Fu, J (2011) Survey of Multispectral Image Fusion Techniques in Remote Sensing Applications Intech:1–22
[6] Song L., Yuchi L., Weichang F., Meirong Z. (2009) A Novel Automatic Weighted Image Fusion Algorithm International Workshop on Intelligent Systems and Applications, ISA, 2009 :1 – 4
[7] Harris, J.R., Murray R., Hirose T. (1990) IHS transform for the integration of radar imagery with other remotely sensed data Photogrammetric Engineering and Remote Sensing, Vol. 56, No. 12:1631-1641.
[8] Gillespie A. R., Kahle A. B., Walker R. E. (1987) Colour enhancement of highly correlated images-II: Channel ratio and chromaticity transformation techniques Remote Sensing of Environment, 22:343–365
[9] Naidu V. P. S., Rao J. R. (2008) Pixel-level Image Fusion using Wavelets and Principal Component Analysis Defence Science Journal, Vol. 58, No. 3: 338-352
[10] Shutao L. (2013) Image Fusion with Guided Filtering IEEE Transactions On Image Processing, Vol. 22, No. 7
[11] Sanju Kumari, Mahesh M., Srikant L. (2014) Image Fusion Techniques Based on Pyramid Decomposition International Journal of Artificial Intelligence and Mechatronics, 2014,Volume 2, Issue 4, ISSN 2320 :5121
[12] Simrandeep S., Narwant S., Grewal, Harbinder S. (2013) Multi-resolution Representation of Multifocus Image Fusion Using Gaussian and Laplacian Pyramids International Journal of Advanced Research in Computer Science and Software Engineering, Volume 3, Issue 11, ,ISSN: 2277 128X
[13] Burt P., Adelson E. (1983) Laplacian pyramid as a compact image code IEEE Transactions on Communications, Vol.31, No. 4
[14] Olkkonen, H., Pesola P. (1996) Gaussian Pyramid Wavelet Transform for Multiresolution Analysis of Images Graphical Models and Image Processing, vol. 58: 394- 398,
[15] Burt P. (1992) A gradient pyramid basis for pattern selective image fusion the Society for Information Displays (SID) International Symposium Digest of Technical Papers, Vol. 23:467-470
[16] Toet, A. (1996) Image fusion by a ratio of low-pass pyramid Pattern Recognition Letters 9: 245-253
[17] Anderson H. A. (1987) Filter-subtract-decimate hierarchical pyramid signal analyzing and synthesizing technique U.S. Patent 718 104
[18] Ramac L. C., Uner M. K., Varshney P. K. (1998) Morphological filters and wavelet based image fusion for concealed weapon detection, Proceedings of SPIE, Vol.3376.
[19] Rajiv S., Ashish K. (2013) Multiscale Medical Image Fusion in Wavelet Domain , Hindawi Publishing Corporation, The Scientific World Journal, Article ID 521034, http://dx.doi.org/10.1155/2013/521034
[20] Pajares G., Dela J. M. (2004) A wavelet – based image fusion tutorial, Pattern Recognition Journal, vol.37,no.9, Elsevier:1855–1872
[21] Burrus C. S., Gopinath R. A., Guo H., Odegard J. E., Selesnick I. W. (1998) Introduction to Wavelets and Wavelet Transforms: A Primer, PrenticeHall, Upper Saddle River, NJ, USA
[22] Unserand M. T. (2003) Wavelet theory demystified, IEEE Transactions on Signal Processing, vol.51, no.2:470–483
[23] Shivsubramani K. , Soman K. P. (2010) Implementation and Comparative Study of Image Fusion Algorithms, International Journal of Computer Applications (0975 – 8887) Volume 9– No.2
[24] Somkait U., Pradab Y., Suwut T.,Pusit B. (2011) Multiresolution Edge Fusion using SWT and SFM, Proceedings of the World Congress on Engineering, London, U.K. ,Vol II: 6 – 8
[25] Pusit B., Wirat R., Somkait U. (2009) Multi-Focus Image Fusion based on Stationary Wavelet Transform, 2009 International Conference on Electronic Computer Technology. 978-0-7695-3559-3/09
[26] Kekre H. B., Athawale A., Dipali S. (2010) Algorithm to Generate Kekre’s Wavelet Transform from Kekre’s Transform, International Journal of Engineering Science and Technology, Vol. 2(5):756-767
[27] Kekre H. B., Sarode T., Dhannawat R. (2012) Implementation and Comparison of different Transform Techniques using Kekre's Wavelet Transform for Image Fusion, International Journal of Computer Applications, Vol. 44, No. 10:41-48.
[28] Kekre H.B., Sarode T., Thepde S. (2011) Inception of Hybrid Wavelet Transform using Two Orthogonal Transforms and It’s use for Image Compression, (IJCSIS) International Journal of Computer Science and Information Security,Vol. 9, No. 6
[29] Kekre H. B., Sarode T., Dhannawat R.(2013) Kekre’s Hybrid Wavelet Transform Technique with DCT, Walsh, Hartley and Kekre’s Transform for Image Fusion, International Journal of Computer Engineering & Technology,Vol 4,No .1:195-202.
[30] Kekre H. B., Sarode T., Dhannawat R. (2012) Image Fusion Using Kekre’s Hybrid Wavelet Transform, International Conference on Communication, Information & Computing Technology (ICCICT), Mumbai, India
[31] Zhang Z., Blum R.S.(1999) A categorization of multiscale-decomposition based image fusion schemes with a performance study for a digital camera application, Proc. IEEE 87 (8) 1315–1326.
[32] Lewis J.J., Callaghan R.J.O., Nikolov S.G., Bull D.R.,

Canagarajah N. (2007) Pixel- and region-based image fusion with complex wavelets, Inf. Fus. 8 (2): 119–130
[33] Nencini F., Garzelli A., Baronti S., Alparone L. (2007) Remote sensing image fusion using the curvelet transform, Special Issue on Image Fusion: Advances in the State of the Art,Inf. Fus. 8 (2): 143–156.
[34] Do M.N.,Vetterli M. (2002) Contourlets: a directional multi-resolution image representation, Proceedings of IEEE International Conference on Image Processing, vol. 1:357–360.
[35] Li T., Wang Y. (2011) Biological image fusion using a NSCT based variable-weight method, Inf. Fus. 12 (2): 85–92.
[36] Wang L., Li B., Tian L. (2014) Multi-modal medical image fusion using the inter-scale and intra-scale dependencies between image shift-invariant shearlet co- efficients, Inf. Fus. 19 (1):20–28.
[37] Farbman Z., Fattal R., Lischinski D., Szeliski R. (2008) Edge-preserving decompositions for multi-scale tone and detail manipulation, ACM Trans. Graph. 27 (3)67:1–67:10.
[38] Hu J., Li S. (2012) The multiscale directional bilateral filter and its application to multisensor image fusion, Inf. Fus. 13 (3):196–206.
[39] Zhou Z., Wang B., Li S., Dong M. (2016) Perceptual fusion of infrared and visible images through a hybrid multi-scale decomposition with gaussian and bilateral filters, Inf. Fus. 30 (1):15–26.
[40] Wang Q., Li S. , Qin H. , Hao A. (2015) Robust multi-modal medical image fusion via anisotropic heat diffusion guided low-rank structural analysis, Inf. Fus. 26(1):103–121.
[41] Redondo R., Roubek V, Fischer S., Cristbal G. (2009) Multifocus image fusion using the log-gabor transform and a multisize windows technique, Inf. Fus. 10 (2):163–171.
[42] Yang S.,Wang M., Jiao L. (2012) Fusion of multispectral and panchromatic images based on support value transform and adaptive principal component analysis, Inf. Fus. 13(3): 177–184.
[43] Zheng S., Shi W.Z., Liu J., Zhu G.X., Tian J.W. (2007) Multisource image fusion method using support value transform, IEEE Trans. Image Process. 16 (7): 1831–1839.
[44] Naidu V. P. S. (2012) Discrete Cosine Transform based Image Fusion Techniques, Journal of Communication, Navigation and Signal Processing,Vol. 1, No. 1:35-45
[45] [dataset] SpineWeb online database containing dataset 1-Spine CT and MR of same patient http://spineweb.digitalimaginggroup.ca/

Authors Profile

Ms B.N. Palkar has received B.E (Computer science and engineering) in 2001, M.E (Computer) from Mumbai University in 2008. She has more than 16 years of experience in teaching. Currently working as associate professor in Department of Computer Engineering at K.J. Somaiya College of engineering, Mumbai. Her areas of interest are Image processing,, Database management systems, Compiler construction.

Mr D. Mishra has received his BE (Computer Engg) degree from University of Mumbai. He completed his M.E. (Computer Engg) from Thadomal shahani Engg. College, Mumbai, University of Mumbai. He received PhD from NMIMS university. He currently works as Professor in Computer Engineering department of Mukesh Patel School of Technology Management and Engineering, SVKM’s NMIMS University, Mumbai, INDIA. His areas of interests are Image Processing, Operating systems, Information Storage and Management.